A Multi Agent Distributed Sensing Architecture with Application to Planetary Cliff Exploration

Vivek A. Sujan, Steven Dubowsky
Department of Mechanical Engineering,
Massachusetts Institute of Technology,
Cambridge, MA 02139

Terry Huntsberger, Hrand Aghazarian, Yang Cheng, Paul Schenker
Mobility System Concept Development Section,
Jet Propulsion Lab, California Institute of Technology,
Pasadena, CA 91109

Abstract— Future planetary exploration missions will use cooperative robots to explore and sample rough terrain. To succeed robots will need to cooperatively acquire and share data. Here a cooperative multi-agent sensing architecture is presented and applied to the mapping of a cliff surface. This algorithm efficiently repositions the systems' sensing agents using an information theoretic approach and fuses sensory information using physical models to yield a geometrically consistent environment map. This map is then distributed among the agents using an information based relevant data reduction scheme. Experimental results for cliff face mapping using the JPL Sample Return Rover (SRR) are presented. The method is shown to significantly improve mapping efficiency over conventional methods.

I. INTRODUCTION

To date planetary robots missions have been limited to moving over rather benign terrain [16]. These systems are not capable of exploring highly irregular terrain such as cliff surfaces that are potentially geologically rich and hence very interesting for planetary science [3, 8]. To succeed robot teams working cooperatively to acquire and share data have been proposed [20]. Here an efficient cooperative multi-agent algorithm for the visual exploration of unknown environments is proposed. This algorithm repositions the systems' sensors using an information theoretic approach and fuses available sensory information from the agents using physical models to yield a geometrically consistent environment map while minimizing the motions of the robots over the hazardous surfaces. This map is distributed among the agents using an information based relevant data reduction scheme. Thus, the experiences (measurements) of each robot become part of the collective experience of the multi-agent team.

The algorithm has been applied in this study to a team of four robots to cooperatively explore a cliff surface. Figure 1 shows schematically four cooperative robots working in an unstructured field environment to. One robot (Cliff-bot) is lowered down a cliff face on tethers. Two robots (Anchorbots) act as anchor points for the tethers. A fourth robot, RECON-bot (REmote Cliff Observer and Navigator) provides mobile sensing. All the robots are equipped with a limited sensor suite, computational power and communication bandwidths. The Cliff-bot, usually the lightest system, may be equipped with primarily a science sensor suite, and limited sensors for navigation. The RECON-bot, serves to observe the environment to be traversed by the Cliff-bot and communicates the data relevant for navigation to the Cliff-bot. The RECON-bot has an independently mobile camera and other onboard sensors to map and observe the environment. Rocks, outcroppings, other robots, etc. limit sensing and sensor placement resulting in uncertainties and occlusions (see Figure 2). There is significant uncertainty the robots' locations and poses with respect to the environment. Due to these limitations and uncertainties it is difficult or impossible for all robots to independently measure the environment to control the system.

Environment mapping by mobile robots falls into the category of Simultaneous Localization and Mapping (SLAM). In SLAM a robot is localizing itself as it maps the environment. Researchers have addressed this problem for well-structured (indoor) environments and have obtained important results [1, 2, 4, 5, 6, 9, 10, 11, 21, 22, 23, 24]. These algorithms have been implemented for several different sensing methods, such as camera vision systems [5, 7, 14], laser range sensors [22, 23], and ultrasonic sensors [1, 6, 11]. Sensor movement/placement is usually done sequentially (raster scan type approach), by following topological graphs or using a variety of *greedy* algorithms that explore regions only on the extreme edges of the known environment [1, 6, 10, 11, 15, 23, 24]. Geometric descriptions of the environment is modeled in several ways, including generalized cones, graph models and voronoi diagrams, occupancy grid models, segment models, vertex models, convex polygon models [6, 10]. The focus of these works is accurate mapping. They do not address mapping efficiency. They also generally assume that the environment is effectively flat (e.g. the floor of an office or a corridor) and readily traversable (i.e. obstacles always have a route around them) [1, 21, 6, 10, 12, 24] and have not been applied to robot teams working in rough planetary environments. Also, prior work has not addressed optimizing the communication between agents for both multi-agent planning and cooperative map-building.

To achieve the localization function landmarks and their relative motions are monitored with respect to the vision

systems. A number of localization schemes have been implemented, including topological generalized voronoi graphs and global topological maps [6, 10, 22, 23], extended Kalman filters [1, 11, 14], and robust averages [14]. Although novel natural landmark selection methods have been proposed [7, 19], most SLAM architectures rely on identifying landmarks as corners or edges in the environment [1, 5, 6, 10, 11, 23]. This works best in well-structured (indoor) environments. Human intervention also has been used to identify landmarks [21].

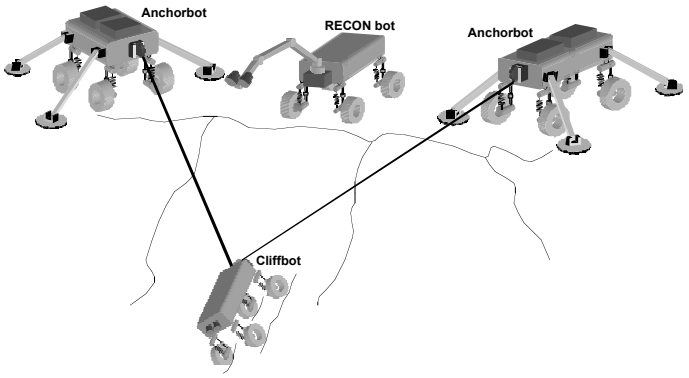

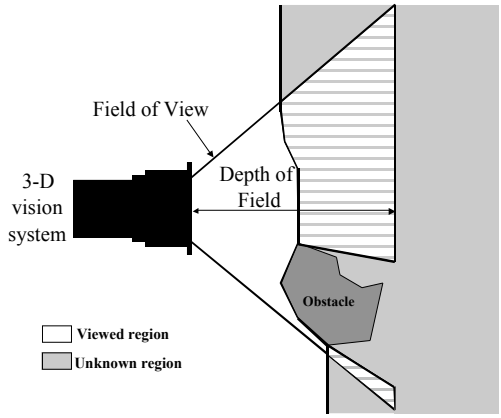

Figure 1: Schematic for a cooperative robot cliff descent **Figure 2: Sensing limitations due to occlusions**

This paper presents a cooperative multi-agent algorithm for the visual exploration of an unknown environment. The basic algorithm is shown in see Figure 3 [20]. This algorithm fuses sensory information from one or multiple agents using physical sensor/robot/environment maps to yield geometrically consistent surrogate information in lieu of missing data due to the environment, task, robot and sensor uncertainties. The system efficiently repositions its' sensors using an information theoretic approach so as to optimally fill in uncertain/unknown regions of the environment map, based on maximizing the expected new information obtained. The information obtained from this process is distributed to the systems' agents. The information is used by the control and planning architecture. Thus a common environment map is built by fusing the data available from the individual robots, providing improved accuracy and knowledge of regions not visible by all robots.

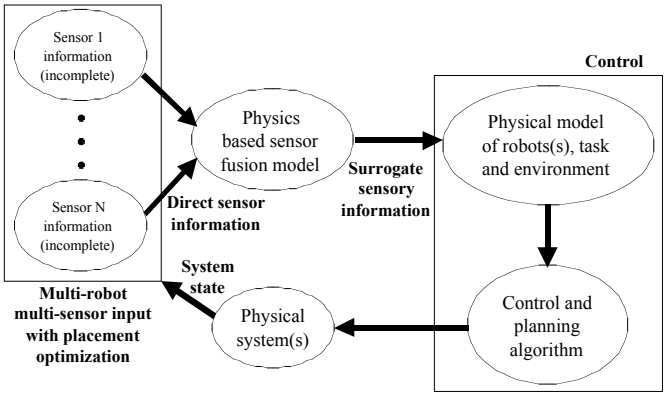

Figure 3: An architecture for multi-robot cooperative sensing

In this paper the algorithm is applied to a cliff surface exploration robot team as described above. In this application the sensing agent is the JPL Sample Return Rover (SRR) which optimally surveys the cliff surface and transmits the information to other agents. Experimental results compare the Model and Information Theory based Sensing And Fusion ExploreR (MIT-SAFER) architecture to conventional raster (or sequential) sensing schemes. The algorithm details are developed and results presented below.

II. MIT-SAFER ANALYTICAL DEVELOPMENT

In general for each sensing agent the algorithm consists of four steps. See Figure 4.

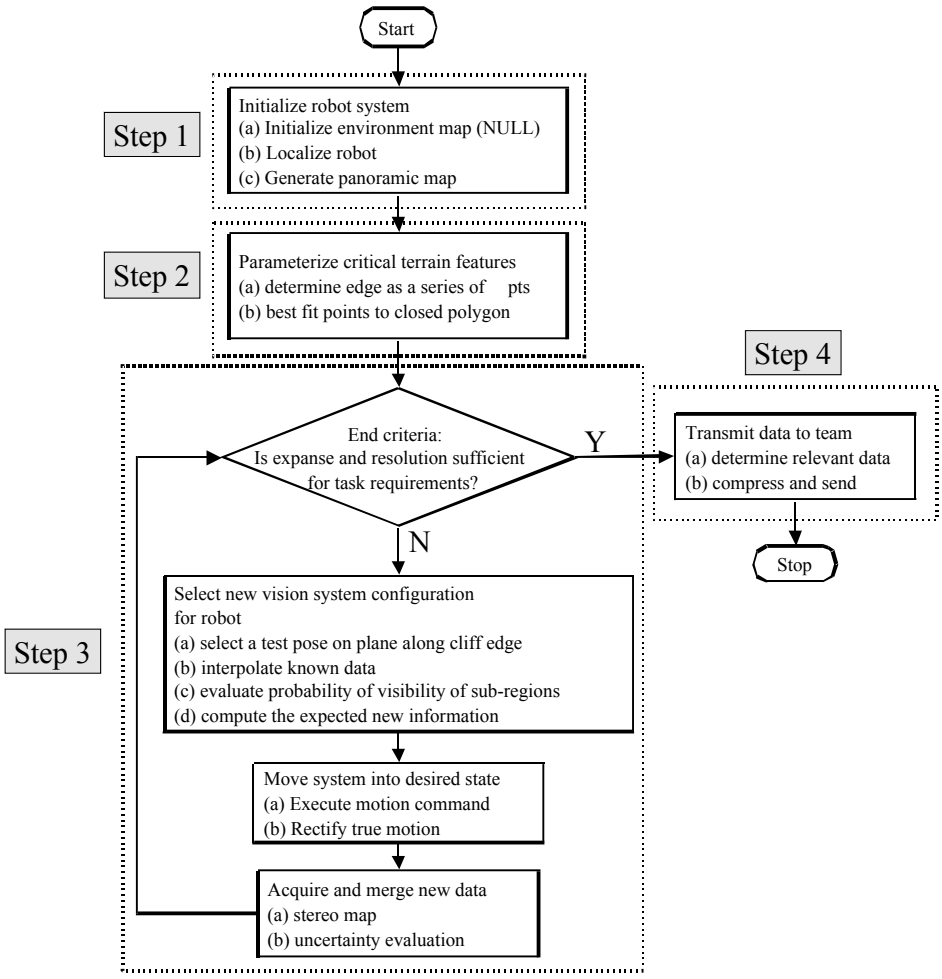

Figure 4: Multi robot environment sensing and distribution flow diagram

Step 1. *System initialization*: Here the environment map is initialized, the robots are localized, and a first map is generated. The environment is mapped to a 2.5D elevation grid i.e. the map is a plane of grid cells where each grid cell value represents the average elevation of the environment at that cell location. All robots contributing to or requiring use of the map are located with respect to the initial map. For the cliff exploration team, these robots include the Cliff-bot and the RECON-bot. Localization may be achieved by either:
(a) Absolute localization—is achieved by mapping a common environment landmark that is visible by all robots or
(b) Relative localization—is done by mapping fiducials on all robots by other robot team members where one robot is selected as the origin. Relative localization is used in this application, with the RECON-bot localizing the Cliff-bot with respect to itself. Then, each agent initially senses the environment.

Step 2. *Critical terrain feature identification*: In some applications, certain regions of the terrain may be critical, requiring early identification and mapping. An example is determining regions of safe travel for the sensing agents. In this application, identification of the cliff edge by the RECON-bot is critical. The edge is parameterized by the edge of a best-fit non-convex polygon of the local terrain. This permits the RECON-bot to move along the cliff edge without falling over it.

Step 3. *Optimum information gathering pose selection*: A rating function is used to determine the next location (position and orientation) of the sensing agent from which to explore the unknown environment. The objective is to acquire as much new information about the environment as possible with every sensing cycle, while maintaining or improving the map accuracy. Hence minimizing the exploration time. The process is constrained by selecting goal points that are not occluded and that can be reached by a collision free feasible path.

The new information (NI) is equal to the expected information of the unknown/partially known region viewed from the sensor pose under consideration. In the case of the cliff surface exploration application, the sensors are CCD

stereo cameras. This is based on the known obstacles from the current environment map, the field of view of the sensor and a framework for quantifying information. Shannon showed that the information gained by observing a specific event among an ensemble of possible events may be described by the following function [18]:

$$H(q_1, q_2, ..., q_n) = -\sum_{k=1}^{n} q_k \log_2 q_k \tag{1}$$

where q_k represents the probability of occurrence for the k^{th} event. This definition of information may also be interpreted as the minimum number of states (bits) needed to fully describe a piece of data. Shannon's emphasis was in describing the information content of 1-D signals. In 2-D the gray level histogram of an ergodic image can be used to define a probability distribution:

$$q_i = f_i / N \text{ for i} = 1...N_{gray} \tag{2}$$

where f_i is the number of pixels in the image with gray level i, N is the total number of pixels in the image, and N_{gray} is the number of possible gray levels. With this definition, the information of an image for which all the q_i are the same—corresponding to a uniform gray level distribution or maximum contrast—is a maximum. The less uniform the histogram, the lower the information.

It has been shown that it is possible to extend this idea of information to a 3-D signal [20]. In this paper this idea is extended to a 2.5D signal—environment elevation map. The new information content for a given sesnor (camera) view pose is given by:

$$H(\text{cam}_{x,y,z,\grave{e}_p,\grave{e}_y}) = -\sum_i \frac{n_{grid}^{max} - n_{grid}^{i}}{n_{grid}^{max}} \left[\frac{P_V^i}{2} \log_2 \frac{P_V^i}{2} + \left(1 - \frac{P_V^i}{2}\right) \log_2 \left(1 - \frac{P_V^i}{2}\right) \right] \tag{3}$$

where H is summed over all grid cells, i, visible from camera pose $\text{cam}_{x,y,z,\grave{e}_p,\grave{e}_y}$; n_{grid}^{i} is the number of environment points measured and mapped to cell i; n_{grid}^{max} is the maximum allowable mappings to cell i; and P_V^i is the probability of visibility of cell i from the camera test pose.

P_V^i is evaluated by computing the likelihood of occlusion of a ray $\mathbf{ray}_{x,y,z}$ using the elevation, $\mathbf{Ob}_{x,y,z}$, and the associated uncertainty, $\sigma_{x,y,z}$, at all cells lying along this ray path shot through each position in the environment grid to the camera center. This is given by:

$$P_V^i = \left[\frac{1}{2} \left[\text{sgn}(\mathbf{ray}_z - \mathbf{Ob}_z) \cdot \int_0^{(\mathbf{ray}_z - \mathbf{Ob}_z)} \frac{1}{\sigma_z \sqrt{2\pi}} \exp\left[-\frac{z^2}{2\sigma_z} \right] dz + 0.5 \right] \right]_{-\sigma_x} \tag{4}$$

This definition for NI has an intuitively correct form. Regions with higher visibility and associated higher level of unknowns yield a higher expected NI value. Higher occlusions or better known regions result in lower expected NI values.

During the mapping process some regions that are expected to be visible may not be, because of sensor characteristics (e.g. lack of stereo correspondence due to poor textures or lighting conditions), and inaccuracies in the data model (e.g. expected neighboring cell elevations and uncertainties—occlusions). However, after repeated unsuccessful measurements of cells expected to be visible, it becomes more likely that sensor characteristics are the limitation. This is represented as a data quality function that reduces as the number of unsuccessful measurements of the visible cell increases. The probability of visibility of the cell i, P_V^i, is pre-multiplied by a "interest function", I.F., for the cell i given at the k^{th} unsuccessful measurement by:

$$\begin{aligned} \text{I.F.}_i^0 &= 1 \\ \text{I.F.}_i^k &= \frac{1}{e^{\hat{a} P_V^i}} \cdot \text{I.F.}_i^{k-1} \end{aligned} \tag{5}$$

where $\hat{a}$ is a scaling constant determined empirically—larger values result in faster decrease of I.F. Note that cells with low P_V^i resulting in an unsuccessful measurement are not as severly penalized as cells with high P_V^i. Hence occluded regions do not translate to low data quality regions. This permits future "interest" in such regions that may be explored later.

A final step in environment map building is to identify the motion of the camera. This process eliminates robot positioning errors, such as camera motion errors, and vehicle suspension motions, and allows for accurate data fusion. A single spatial point in the base frame, $\bar{r}_i$, is related to the image point (u_i, v_i) in the sensor frame by the 4x4 transformation matrix $\mathbf{g}_{01}$. Spatial points are selected and tracked based on a Forstner interest operator and a homography transform [8].

For motion calibration of a camera $\mathbf{g}_{01}$needs to be identified:

$$\begin{bmatrix} k_i u_i \\ k_i v_i \\ k_i f \\ 1 \end{bmatrix} = g_{01} \cdot \bar{r}_i = \begin{bmatrix} [R_{01}]_{3x3} & \bar{X}_{3x1} \\ 0 & 1 \end{bmatrix} \cdot \begin{bmatrix} r_i^x \\ r_i^y \\ r_i^z \\ 1 \end{bmatrix} \tag{6}$$

where $\mathbf{R}_{01}$ is the rotational matrix, $\bar{X}$ is the translation vector, f is the camera focal length, and k_i is a scaling constant. For computational reasons it is more convenient to treat the 9 rotational components of $\mathbf{R}_{01}$ as independent, rather than a transcedental relation of 3 independent parameters. Each spatial point gives three algebraic equations, but also introduces a new variable, k_i—multiplicative constant to extend the i^{th} image point vector $(u,v,f)_i$ to the i^{th} spatial point in the camera coordinate frame. k_i may be found from the disparity pair of the stereo images. For n points we have:

$$u = g_{01} r \begin{bmatrix} k_1 u_1 & k_2 u_2 & \cdots & k_n u_n \\ k_1 v_1 & k_2 v_2 & & k_n v_n \\ k_1 f & k_2 f & & k_n f \\ 1 & 1 & & 1 \end{bmatrix} = g_{01} \begin{bmatrix} r_1^x & r_2^x & \cdots & r_n^x \\ r_1^y & r_2^y & & r_n^y \\ r_1^z & r_2^z & & r_n^z \\ 1 & 1 & & 1 \end{bmatrix} \tag{7}$$

This set of linear equations can be readily solved using conventional techniques. A least mean square error solution is given by:

$$\mathbf{g_{01}} = \mathbf{u}\left(\mathbf{r}^T\mathbf{r}\right)^{-1}\mathbf{r}^T \tag{8}$$

The rotation matrix, $\mathbf{R}_{01}$, and the translation vector, $\bar{X}$, of the camera frame with respect to the base frame are extracted directly from this solution of $\mathbf{g}_{01}$. However, for real measured data and associated uncertainty, a larger number of spatial points are required to more correctly identify the geometric transformation matrix, $\mathbf{g}_{01}$. Given the $(i+1)^{st}$ spatial and image point, from Equation 8, $\mathbf{R}_{i+1}$ and $\bar{X}_{i+1}$ can be obtained. A recursive method is used to determine the mean and covariance of $\bar{X}$ and $\mathbf{R}_{01}$ based on the previous i measurements.

This essentially maintains a measure on how certain the camera motion is with respect to its original configuration (assuming the original configuration is known very precisely with respect to the common reference frame). To obtain an estimate on the position uncertainty of a measured point in the environment, this camera pose uncertainty must be accounted for. The measurement $\bar{z}$ be related to the state vector (actual point position) $\bar{x}$ by a non-linear function, $h(\bar{x})$. The measurement vector is corrupted by a sensor noise vector $\bar{v}$ of known covariance matrix, $\mathbf{Q}$. Assume that the measurement of the state vector $\bar{x}$ is done multiple times. In terms of the current measurement, a Jacobian matrix of the measurement relationship evaluated at the current state estimate may be obtained. The state (or positition) may then be estimated with the Extended Kalman Filter. Using this updated value for both the measured point $\bar{x}$ and the absolute uncertainty $\mathbf{P}$, the measured point may then be merged with the current envrionment map using equations 2 and 4.

In addition to maximizing information acquisition, it is also desirable to minimize travel distance and maintain/improve the map accuracy, while being constrained to move along feasible paths. A Euclidean metric in configuration space, with individual weights α_i on each degree of freedom of the camera pose $\bar{c}$, is used to define the distance moved by the camera:

$$d = \left[\sum_{i=1}^{n} \alpha_i (c_i - c'_i)^2\right]^{1/2} \tag{9}$$

where $\bar{c}$ and $\bar{c}'$ are vectors of the new and current camera poses respectively. Here α_i is set to unity. In general this parameter reflects the ease/difficulty in moving the vision system in the respective axis. Map accuracy is based

on the accuracy of localization of each sensing agent. This may be obtained by adding the localization error of the agent along the path to the target. Paths containing more promising fiducials for localization result in higher utility in determining both the goal location and the path to the goal. The new information, the travel distance and the net improvement of map accuracy is combined into a single utility function that may be optimized to select the next view pose.

Step 4. *Map distribution:* As each agent maps and fuses an environment section to the environment map, it needs to distribute this updated map among the other agents. This is required so that each agent may optimally plan its next move. Once completed, the environment map needs to be distributed to the team. For example, to explore the cliff, after the RECON-bot has developed the geometrical cliff surface map, it needs to transfer this to the Cliff-bot for task execution (e.g. science instrument placement).

Due to communication bandwidth limitations of NASA present and near-term planetary exploration robots, an appropriate data transfer algorithm needs to be developed. These communication limitations would be exacerbated with many cooperating agents. Thus successful communication requires the reduction of the data set into relevant data i.e. only communicate data that is necessary for task execution.

The data reduction algorithm used here breaks down the environment map into a *quadtree of interest regions.* This is achieved by first reducing the entire elevation map with adaptive decimation. This removes highly insignificant objects, such as small pebbles. The resulting data set is divided into four quadrants. The information content of each quadrant is evaluated using Equations (1) and (2). This information content reflects the amount of variation in the terrain quadrant (where higher information content signifies higher variation in the terrain). Quadrants with high information content are further divided into sub-quadrants and the evaluation process is continued. Once it is determined that a quadrant does not require further subdivision, an average elevation value of the particular quadrant is used for transmission (rather than the elevation of all grid cells within that quadrant). This cutoff threshold of information is based on a critical robot physical parameter (e.g. the wheel diameter). This results in a significantly reduced data set known as the *quadtree of interest regions*. Conventional lossless compression schemes may then be applied to the reduced data set to further reduce the number of transmission bits. The flow diagram of this process is given in Figure 5.

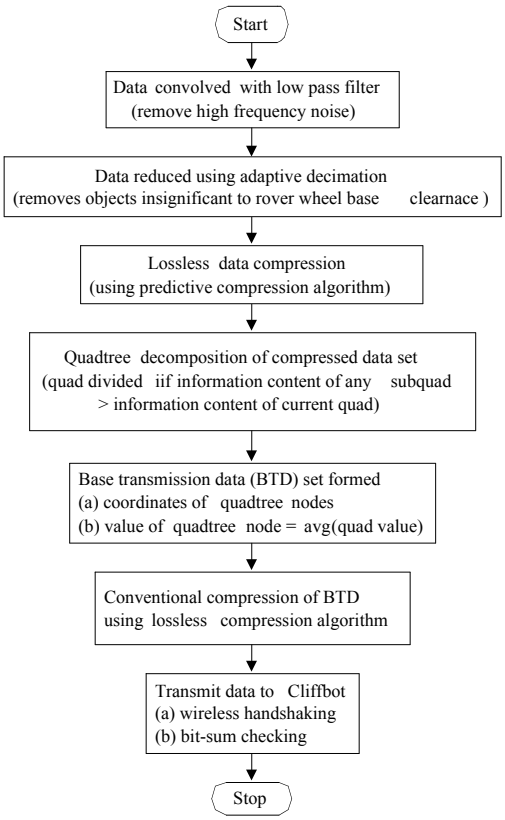

Figure 5: Inter-robot communication flow diagram

III. EXPERIMENTAL RESULTS

The basic MIT-SAFER algorithm was applied to the cooperative exploration of cliff surfaces by a team of four robots. The JPL Sample Return Rover (SRR) served as the RECONbot for this application. The SRR is a four-wheeled mobile robot with independently steered wheels and independently controlled shoulder joints. It carries a stereo pair of cameras mounted on a three DOF articulated manipulator. The SRR is equipped with a 266 MHz PC-104 computer platform, operating with VX-Works. Five mapping techniques, including the one developed above, were implemented. These were: (Method 1) raster scanning without yaw, (Method 2) raster scanning with yaw, (Method 3) information based environment mapping with cliff edge assumed to be a straight line segment, (Method 4) information based environment mapping with cliff edge approximated as a non-convex polygon, (Method 5) information based environment mapping with interest function and cliff edge approximated as a non-convex polygon. The first two methods reflect commonly used environment mapping schemes. The latter three reflect with increased complexity the algorithm developed here.

The experimental setup for the first study in the Planetary Robotics Lab (PRL) at JPL is shown in Figure 6. A recessed sandpit containing several rock piles is mapped. The edge of the sandpit, a vertical drop, acts as the cliff edge. This limits the motion of the RECON-bot to lie in the flat plane behind the cliff edge (see Figure 6). Figure 7 shows the number of environment grid cells explored as a function of the number of stereo imaging steps. From this experimental study, the improved efficiency of the method presented in this paper over conventional raster scanning methods can be seen, with an order of magnitude more points being mapped by Method 5 over those returned from Method 1 for the same number of stereo imaging steps. A significant improvement in efficiency can be seen while progressing from Method 3 to Method 5. In Method 4, by parameterizing the cliff edge, the rover is able to follow the edge more aggressively, thus covering a larger variety of view points.

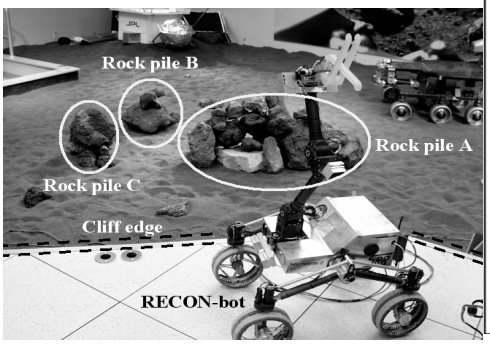

Figure 6: Experimental laboratory setup

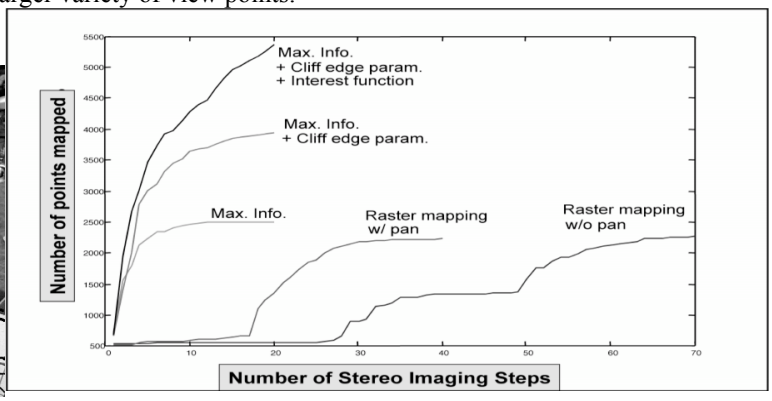

Figure 7: Amount of environment explored

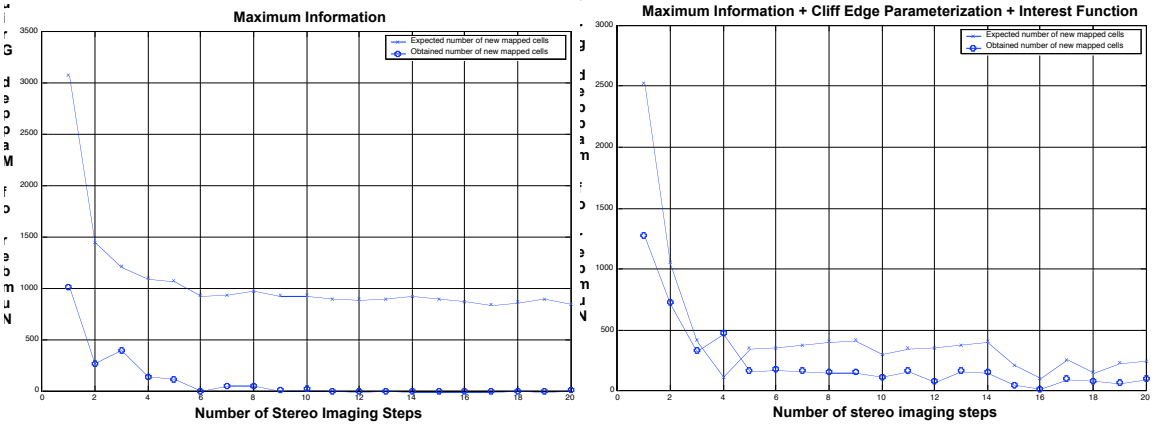

(a) Method 3 **(b) Method 5**

Figure 8: Comparison of the number of expected new mapped cells verses the number obtained

Further, it is observed that the left region of the sandpit in Figure 6 yields poor data (due to lack of stereo correspondence). Since this region is expected have high information content (due to lack of occlusions), the algorithm in Method 3 tends to converge to view points looking in that direction. However, in Method 5, the algorithm concludes that the data quality is poor and eventually loses interest in this region. This is seen in Figure 8

that shows the number of expected environment grid cell measurements as opposed to the number obtained. In method 5, there is reasonable agreement. However, in method 3, while the expected number of measurements is significant, the obtained number of grid cell measurements drops off to zero.

Field tests were conducted near the Tujunga Dam in Tujunga, CA on a natural cliff face with a vertical slope of ~75°. This setup seen in Figure 9. This is the physical realization of the conceptual description provided in section I of a team of four cooperating robots exploring a cliff surface. Due to time constraints, experimental tests could only be run for Method 4 using the maximum information content and Method 5 using the maximum information content with interest function. The results of the study for 10 imaging steps is shown in Figure 10. Figure 11 shows part of the cliff surface and its corresponding map. Of particular interest is the rock jumble to the Cliffbot, which may choose to avoid it during traversal.

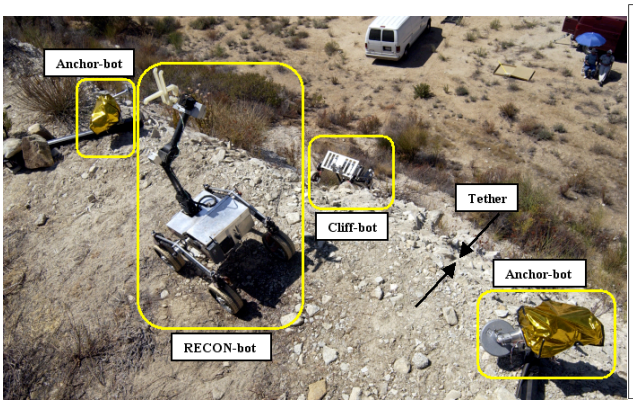

Figure 9: Experimental field system setup

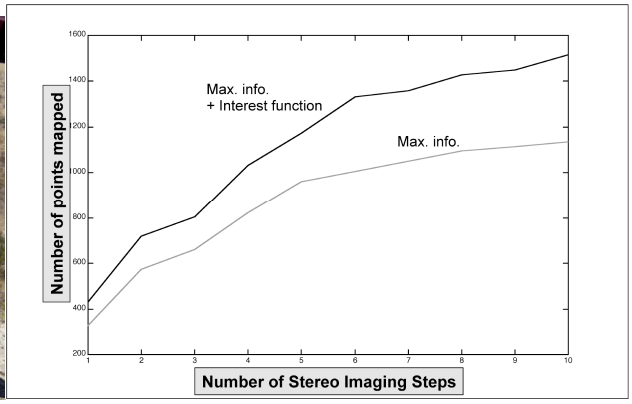

Figure 10: Amount of environment explored

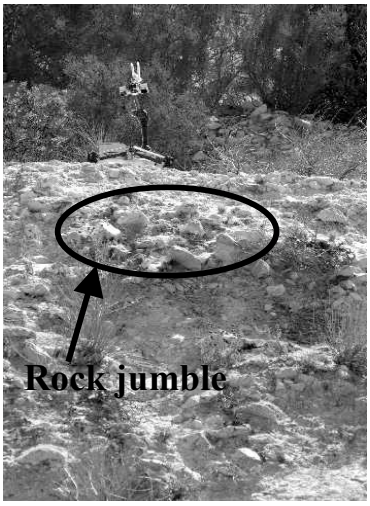

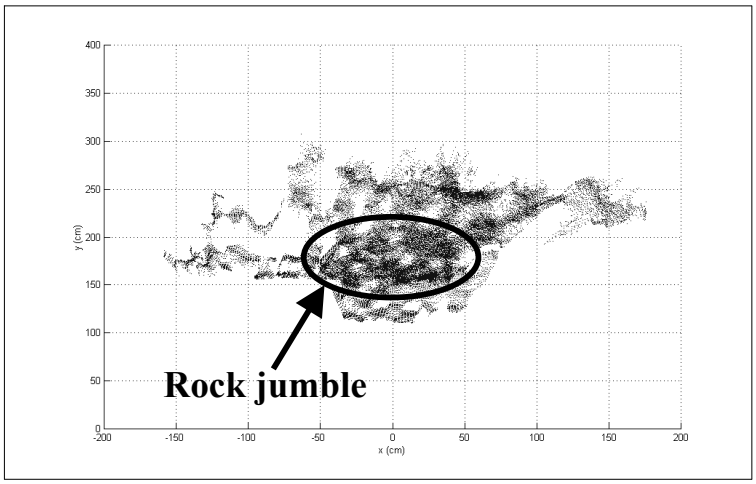

(a) View of RECONbot mapping the cliff **(b) Overhead view of surface mapped**

Figure 11: Tajunga dam cliff site

These results demonstrate the effectiveness of the multi-agent environment mapping architecture developed in this paper. To demonstrate the effectiveness of the map reduction and distribution algorithm for robots in real Mars field environments, 32 different elevation maps of fixed dimensions, based on the statistics of Viking I/II Mars lander data were tested. The data of each elevation map was reduced with respect to a robot with varying wheel diameter. To compare the data reduction, a terrain variation parameter, dH, is defined as the terrain elevation variation normalized by the robot wheel diameter. Thus it is expected that robots with smaller wheel diameters (higher dH) require a greater amount of terrain detail for navigation, than those with larger wheel diameters for the same terrain map. Figure 12 confirms this expectation. It shows the data reduction factor as a function of dH using the algorithm described above (without conventional lossless compression added at the end). The variation at each data point represents the variation in data reduction expected for a given elevation map.

An example of this data reduction process is shown in Figure 13. It compares the grayscale elevation map before and after the data reduction process—lighter regions indicate higher elevations. For this example, a data reduction factor of approximately 10 was achieved with a dH = 8. Although visually the left and right images may appear the same, closer inspection reveals regions in the transmitted image (such as the bottom right corner) to contain very little information content. This indicates that the region in the original elevation contained insignificant terrain variation with respect to the particular wheel diameter. However, other regions such as the boulders, indicated in the original elevation map, that are critical with respect to the wheel diameter, are faithfully transmitted. It is seen that using this method, significant data reduction can be achieved while maintaining the overall map structure. Although, this is applied to a 2.5D environment elevation map here, the algorithm is directly applicable to 3D maps.

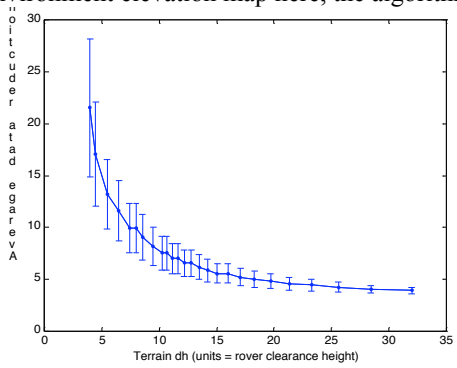

Figure 12: Elevation map data reduction for transmission as a function of wheel diameter variation

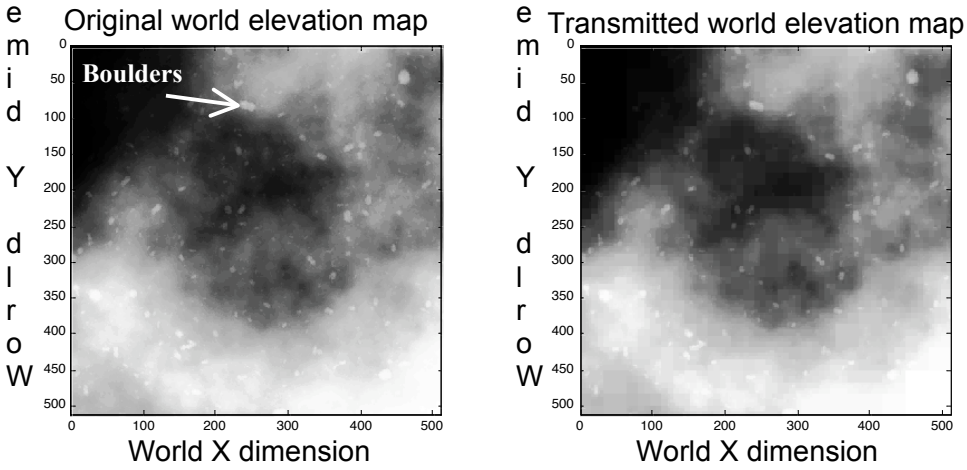

Figure 13: The original (left) and the process/transmitted (right) environment elevation maps.

IV. CONCLUSIONS

This paper has presented a cooperative multi-agent distributed sensing architecture. This algorithm efficiently repositions the systems' sensors using an information theoretic approach and fuses sensory information from the agents using physical models to yield a geometrically consistent environment map. This map is then distributed using an information based relevant data reduction scheme for communication. The architecture is proposed for a team of robots cooperatively interacting to explore a cliff face. Experimental results using the JPL Sample Return Rover (SRR) have been presented. This single rover acts as a surveyor, optimally generating a map of the cliff face. The method is shown to significantly improve the environment mapping efficiency. The algorithm shows additional mapping efficiency improvement when an interest function is included. This function measures the data quality in the environment. Future work includes implementation and testing of the inter-robot communication algorithm on the experimental platform.

V. ACKNOWLEDGEMENTS

The authors would like to acknowledge the support of the Jet Propulsion Laboratory, NASA under contract number 1216342.

VI. REFERENCES

[1] Anousaki, G.C., Kyriakopoulos, K.J. *Simultaneous localization and map building for mobile robot navigation.* IEEE Robotics & Automation Magazine , Volume: 6 Issue: 3 , Sept. 1999 Page(s): 42 –53

[2] Asada, M. *Map building for a mobile robot from sensory data*. IEEE Trans. on Systems, Man, and Cybernetics. Vol. 37, no. 6, Nov/Dec 1990.

[3] Baumgartner, E.T., P. S. Schenker, C. Leger, and T. L. Huntsberger. *Sensor-fused navigation and manipulation from a planetary rover*. Proceedings SPIE Symposium on Sensor Fusion and Decentralized Control in Robotic Systems, Vol. 3523, Boston, MA, Nov 1998.

[4] Burschka, D. Eberst, C. and Robl, C. *Vision based model generation for indoor environments.* Proceedings of the 1997 IEEE International Conference on Robotics and Automation, Albuquerque, New Mexico, April, 1997

[5] Castellanos, J.A., Martinez, J.M., Neira, J., Tardos, J.D. *Simultaneous map building and localization for mobile robots: a multisensor fusion approach.* Proc. of 1998 IEEE ICRA. Volume: 2, 1998 Page(s): 1244 –1249

[6] Choset, H., Nagatani, K. *Topological simultaneous localization and mapping (SLAM): toward exact localization without explicit localization.* IEEE Trans. on Rob. & Auto., Vol. 17 Iss. 2, Apr. 2001 Pp: 125 –137

[7] Hager, G.D., Kriegman, D., Teh, E., Rasmussen, C. *Image-based prediction of landmark features for mobile robot navigation.* Proceedings of the 1997 IEEE ICRA Volume: 2, Page(s): 1040 –1046

[8] Huntsberger, T.L., G. Rodriguez, and P. S. Schenker. *Robotics: challenges for robotic and human Mars exploration*. Proceedings of ROBOTICS2000, Albuquerque, NM, Mar 2000.

[9] Kruse, E., Gutsche, R., and Wahl, F.M. *Efficient, iterative, sensor based 3-D map building using rating functions in configuration space.* Proceedings of the 1996 IEEE ICRA, Minneapolis, Minnesota, April, 1996.

[10] Kuipers, B., Byun, Y. *A robot exploration and mapping strategy based on semantic hierarchy of spatial representations.* Journal of Robotics and Autonomous Systems 8, 47-63, 1991

[11] Leonard, J.J., Durrant-Whyte, H.F. *Simultaneous map building and localization for an autonomous mobile robot.* IEEE 1991 Int. Wrkshp on Intelligent Robots and Sys. Pp(s): 1442 -1447 vol.3. Nov 3-5, Osaka, Japan.

[12] Lumelsky, V., Mukhopadhyay, S. and Sun, K. *Sensor-based terrain acquisition: the "sightseer" strategy.* Proceedings of the 28th Conference on Decision and Control. Tampa, Florida. December 1989.

[13] Osborn, J.F. *Applications of Robotics in Hazardous Waste Management* Proc. of SME 1989 World Conf. on Robotics Research, Gaithersburg, MD.

[14] Park J., Bolan Jiang, Neumann, U. *Vision-based pose computation: robust and accurate augmented reality tracking.* Proceedings of the 2nd IEEE/ACM Int. Wrkshp. on Augmented Reality, 1999. Page(s): 3 –12

[15] Rekleitis, I., Dudek, G., and Milios, E. *Multi-robot collaboration for robust exploration.* Proceedings of the 2000 IEEE International Conference on Robotics and Automation, San Francisco, CA. April, 2000.

[16] Schenker, P.S., et. al. *New planetary rovers for long-range Mars science and sample return*. Proc. SPIE Symp. on Int. Robots and Comp. Vision XVII: Algorithms, Techniques, and Active Vision, Vol. 3522, Boston, MA, Nov 1998.

[17] Shaffer, G.; Stentz, A. *A robotic system for underground coal mining.* Proc. of 1992 IEEE ICRA. Page: 633 - 638 vol.1

[18] Shannon, C. E. *A mathematical theory of communication.* The Bell System Technical Journal, vol. 27, pp. 379-423, July, 1948.

[19] Simhon, S., Dudek, G. *Selecting targets for local reference frames.* Proceedings of the 1998 IEEE ICRA. Volume: 4, Page(s): 2840 -2845 vol.4

[20] Sujan, V.A. and Dubowsky, S. *Visually Built Task Models for Robot Teams in Unstructured Environments.* Proceedings of the 2002 IEEE ICRA, May 11-15, 2002, Washington, D.C., U.S.A.

[21] Thrun, S., Burgard, W., and Fox, D. *A real-time algorithm for mobile robot mapping with applications to multi-robot and 3D mapping.* Proceedings of the 2000 IEEE ICRA. San Francisco, CA, April, 2000.

[22] Tomatis, N., Nourbakhsh, I., Siegwar, R. *Simultaneous localization and map building: a global topological model with local metric maps*. Proc. of IEEE/RSJ IROS. Vol.: 1, 2001 Pp: 421 –426

[23] Victorino, A.C., Rives, P., Borrelly, J.-J. *Localization and map building using a sensor-based control strategy*. Proc. of IEEE/RSJ IROS, Volume: 2, Page(s): 937 -942 vol.2

[24] Yamauchi, B., Schultz, A., Adams, W. *Mobile robot exploration and map-building with continuous localization.* Proc. of IEEE ICRA 1998. Volume: 4 Page(s): 3715 -3720 vol.4